Computer Assisted Mechanics and Engineering Sciences, 8: 313–324, 2001.

An energy-momentum algorithm for flexible multibody systems with finite element techniques

Juan C. García Orden and Jose M. Goicolea
Department of Continuum Mechanics and Theory of Structures,
Madrid University of Technology, Ciudad Universitaria s/n, 28042 Madrid, Spain

(Received June 30, 2000)

A unified approach for the treatment of the non-linear dynamics of multibody systems (MBS) composed of both rigid and elastic bodies is proposed. Large displacements and rotations, large strains and non-linear elastic material response are considered for the elastic bodies.

The proposed formulation exploits three key ingredients: the use of a dependent set of inertial coordinates of selected points of the system; the use of a basic constraint library enforced through the penalty method; the use of the energy-momentum method to integrate the equations.

The proposed algorithm is set in the framework of a non-conventional finite element formulation, which combine naturally the displacement-based discretisation of the deformable bodies with rigid body mechanics. Two key performance features are achieved. The exact conservation of total momentum and total energy in conservative systems is ensured. The major drawback of the penalty method, namely numerical ill-conditioning that leads to stiff equation systems, is overcome.

1. Introduction

A flexible multibody system is understood as a collection of rigid and deformable bodies acted by different types of loads and linked by different types of joints. These joints can be passive (spherical, cylindrical, prismatic) or active (springs, dampers, etc.).

These models are usually employed when the flexible parts may affect substantially the global dynamic behaviour of the whole system. They are quite common in aerospace and automotive applications.

Rigid bodies are modelled as discrete elements parametrised by a finite set of coordinates, and deformable bodies are represented by continuum media. These deformable bodies are assumed to experience large displacements and strains, and made of materials with hyperlastic behaviour.

The continuum bodies are discretised using the Finite Element Method (F.E.M.) and assembled with the discrete rigid bodies to establish the global system of equations, which is then integrated in time. This formulation sets the basis of a non-conventional finite element technique, with perfect coupling between the dynamic effects of both rigid and deformable parts.

The main goal of the proposed approach is to define a simple and efficient method to treat such systems in long-term simulations, where the total integration time is considerably larger than the longest period of the movement, which typically corresponds to the large-amplitude rigid body motions. In order to accomplish this objective, three key ingredients are employed.

Firstly, the system is parametrised using inertial Cartesian coordinates of selected points: at least four points from each rigid body (in order to build a constant mass matrix) and all nodal points from the deformable bodies. This selection leads to a dependent set of coordinates related through constraint equations.

Secondly, the constraints are enforced using the penalty method. This approach, combined with the specific parametrisation described above, sets the basis for a simple and systematic dynamic formulation based on a single global system of ordinary differential equations.

Because the numerical ill-conditioning introduced in the equations by the penalty method strongly determines the type of time-stepping scheme to be employed, the third and last ingredient of the approach consists in using a energy-momentum method of integration, which can be rigorously designed in the context of general Hamiltonian systems with symmetry. It shows an excellent overall performance in terms of robustness and accuracy. Additionally, the energy-momentum method provides high confidence in the results successfully obtained in long-term simulations, since basic physical magnitudes, such as energy and momentum, are exactly conserved.

It is important to remark that the interest in the energy-momentum method is not restricted to conservative systems. The application of an energy-momentum method to dissipative systems assures that the observed energy dissipation introduced by the underlying physical model is not corrupted by the numerical model.

2. MULTIBODY SYSTEMS COMPOSED BY RIGID BODIES

Consider a collection rigid bodies $\mathcal{B}_R$ and denote by $\boldsymbol{x}$ the spatial coordinates, expressed in an inertial Cartesian reference system, of an arbitrary point of any of the bodies.

The general weak form of the equations of motion takes the form

$$\int_{\mathcal{B}_R} \delta\boldsymbol{x}^{\mathrm{T}} \cdot \ddot{\boldsymbol{x}}\, \rho \,\mathrm{d}V - \int_{\mathcal{B}_R} \delta\boldsymbol{x}^{\mathrm{T}} \cdot \boldsymbol{b}_R \,\mathrm{d}V - \int_{\partial\mathcal{B}_R} \delta\boldsymbol{x}^{\mathrm{T}} \cdot \boldsymbol{t}_R \,\mathrm{d}A = 0 \qquad \forall \delta\boldsymbol{x} \in \mathcal{V} \tag{1}$$

where $\mathcal{V}$ is the finite-dimensional space of the constraint-compatible variations of $\boldsymbol{x}$, $\boldsymbol{b}_R$ is the vector of volumetric load and $\boldsymbol{t}_R$ the vector of concentrated loads applied on the boundary $\partial\mathcal{B}_R$ of the system.

Introducing a parametrisation $\boldsymbol{x} = \boldsymbol{x}(\mathbf{q}_R)$, Eq. (1) can be expressed in terms of the set of coordinates $\mathbf{q}_R \in \mathbb{R}^m$, taking the general form

$$\delta\mathbf{q}_R^{\mathrm{T}} \cdot (\mathbf{M}_R \cdot \ddot{\mathbf{q}}_R - \mathbf{Q}_R) = 0 \tag{2}$$

where $\mathbf{M}_R$ is the mass matrix and $\mathbf{Q}_R(\mathbf{q}_R\,,\,\dot{\mathbf{q}}_R\,,\,t)$ the vector of generalised forces. The specific form of each term in Eq. (2) depends on the selected parametrisation. If $\mathbf{q}_R \in \mathbb{R}^{3N}$ contains Cartesian coordinates of N selected points and the inertial coordinates of an arbitrary point are written as $\boldsymbol{x} = \mathbf{C} \cdot \mathbf{q}_R$, then

$$\mathbf{M}_R = \int_{\mathcal{B}_R} \mathbf{C}^{\mathrm{T}} \cdot \mathbf{C}\, \rho \,\mathrm{d}V,$$

$$\mathbf{Q}_R = \mathbf{C}^{\mathrm{T}} \cdot \boldsymbol{f}_R + \int_{\mathcal{B}_R} \mathbf{C}^{\mathrm{T}} \cdot \boldsymbol{b}_R \,\mathrm{d}V.$$

If each body is defined by at least four points defining a non-zero volume, it can be shown [1] that the mass matrix $\mathbf{M}_R$ is constant.

It is important to remark that the variations $\delta\mathbf{q}_R$ in (2) are not independent. For instance, the definition of a single rigid body by four points such that $\mathbf{q}_R \in \mathbb{R}^{12}$, requires six constant-distance constraints, giving a total of six degrees of freedom. If the body is linked to other bodies, the number of constraints increases. The conclusion is that this parametrisation, even for a single free rigid body, always requires constraints relating the elements of the coordinate vector $\mathbf{q}_R$.

Enforcement of holonomic constraints of the type $\boldsymbol{\Phi} : \mathbb{R}^{3N} \times \mathbb{R} \ni (\mathbf{q}_R\,,\,t) \longmapsto \boldsymbol{\Phi}(\mathbf{q}_R\,,\,t) \in \mathbb{R}^p$ can be accomplished by several methods. Denoting by $\mathbf{f}_\Phi \in \mathbb{R}^{3N}$ the constraint force vector, the following expressions are obtained for different methods [1]:

- *Lagrange multipliers method*

$$\mathbf{f}_\Phi = -\frac{1}{2}(\mathrm{D}\boldsymbol{\Phi})^{\mathrm{T}} \cdot \boldsymbol{\lambda}; \qquad \mathrm{D}\boldsymbol{\Phi} \equiv \frac{\partial \boldsymbol{\Phi}}{\partial \mathbf{q}_R};$$

- *Penalty method*

$$\mathbf{f}_\Phi = -(\mathrm{D}\boldsymbol{\Phi})^{\mathrm{T}} \cdot (\boldsymbol{\alpha} \cdot \boldsymbol{\Phi}); \qquad V_\Phi = \frac{1}{2}\boldsymbol{\Phi}^{\mathrm{T}} \cdot (\boldsymbol{\alpha} \cdot \boldsymbol{\Phi});$$

- *Augmented Lagrangian*

$$\mathbf{f}_\Phi = -(\mathrm{D}\boldsymbol{\Phi})^{\mathrm{T}} \cdot (\boldsymbol{\alpha} \cdot \boldsymbol{\Phi}) + (\mathrm{D}\boldsymbol{\Phi})^{\mathrm{T}} \cdot \boldsymbol{\lambda}^*; \qquad \boldsymbol{\lambda}^*_{i+1} = \boldsymbol{\lambda}^*_i + \boldsymbol{\alpha} \cdot \boldsymbol{\Phi}_{i+1}.$$

It is important to notice that the penalty method introduces naturally the constraint force from a potential V_Φ. This fact has relevance in the formulation of the energy-momentum method used to integrate the equations of motion in time.

Introducing the constraint equations with the penalty method in Eq. (2), the following expression is obtained for the weak formulation,

$$\delta\mathbf{q}_R^{\mathrm{T}} \cdot \Big(\mathbf{M}_R \cdot \ddot{\mathbf{q}}_R - \underbrace{(\mathrm{D}\boldsymbol{\Phi})^{\mathrm{T}} \cdot (\boldsymbol{\alpha} \cdot \boldsymbol{\Phi})}_{\mathbf{f}_{\Phi_R}} - \mathbf{Q}_R\Big) = 0 \qquad \forall \delta\mathbf{q}_R \in \mathcal{V}^{3N} \tag{3}$$

where $\delta\mathbf{q}_R \in \mathcal{V}^{3N}$ are truly independent and can be eliminated.

3. Deformable bodies and global rigid-deformable equations

Consider a single deformable body $\mathcal{B}_E$, with boundary $\partial\mathcal{B}_R$, under volumetric $\boldsymbol{b}_E$ and concentrated $\boldsymbol{t}_E$ loads, and with holonomic constraints $\boldsymbol{\Phi}_E$ acting over a domain $\partial_\Phi\mathcal{B}_E$. The weak form of the equations of motion can be expressed in terms of the virtual work of the inertia, internal, external and constraint forces,

$$\underbrace{\int_{\mathcal{B}_E} \delta\boldsymbol{x}^{\mathrm{T}} \cdot \ddot{\boldsymbol{x}}\, \rho\, \mathrm{d}V}_{\delta\Pi_{\mathrm{iner}}} - \underbrace{\int_{\mathcal{B}_{E_0}} \mathrm{D}(\delta\boldsymbol{x})^{\mathrm{T}} \cdot \boldsymbol{F}\boldsymbol{S}\, \rho\, \mathrm{d}V_0}_{\delta\Pi_{\mathrm{int}}}$$
$$\underbrace{- \int_{\mathcal{B}_E} \delta\boldsymbol{x}^{\mathrm{T}} \cdot \boldsymbol{b}_E\, \rho\, \mathrm{d}V - \int_{\partial\mathcal{B}_E} \delta\boldsymbol{x}^{\mathrm{T}} \cdot \boldsymbol{t}_E\, \mathrm{d}A}_{\delta\Pi_{\mathrm{ext}}} - \underbrace{\int_{\partial_\Phi\mathcal{B}_E} \delta\boldsymbol{x}^{\mathrm{T}} \cdot (\mathrm{D}\boldsymbol{\Phi}_E)(\boldsymbol{\alpha}\boldsymbol{\Phi}_E)\, \mathrm{d}A}_{\delta\Pi_{\mathrm{constr}}} = 0, \tag{4}$$

with $\delta\boldsymbol{x} \in \mathcal{V}$, where $\mathcal{V}$ is the infinite-dimensional space of all arbitrary variations of $\boldsymbol{x}$. In Eq. (4), $\mathcal{B}_{E_0}$ is the undeformed configuration, $\boldsymbol{F}$ is the deformation gradient tensor and $\boldsymbol{S}$ is the second Piola–Kirchhoff stress tensor. Constraints are enforced by the penalty method.

Continuum bodies are discretised using a standard displacement-based finite element interpolation,

$$\boldsymbol{x} = \mathbf{N} \cdot \mathbf{q}^e_E. \tag{5}$$

In the expression above $\mathbf{N}$ is the interpolation matrix, calculated from the shape functions, and $\mathbf{q}^e_E$ is a vector containing the inertial Cartesian coordinates of the nodes. For isoparametric elements, positions and displacements are interpolated in the same way, to yield

$$\delta\boldsymbol{x} = \mathbf{N} \cdot \delta\mathbf{q}^e_E. \tag{6}$$

Introducing the parametrisation given by relations (5), (6) in (4), the contribution of element Ω^e has the form

$$(\delta\mathbf{q}_{\mathrm{E}}^e)^{\mathrm{T}} \cdot \Big(\underbrace{\int_{\Omega^e} \rho \mathbf{N}^{\mathrm{T}} \cdot \mathbf{N}\, \mathrm{d}V}_{\mathbf{M}_{\mathrm{E}}^e} \ddot{\mathbf{q}}_{\mathrm{E}}^e - \underbrace{\int_{\Omega_0^e} \mathbf{B}\boldsymbol{S}^e\, \mathrm{d}V_0}_{\mathbf{f}_{\mathrm{int}}^e} - \mathbf{Q}_{\mathrm{E}}^e \Big)$$

where $\mathbf{M}_E^e$ and $\mathbf{f}_{\mathrm{int}}^e$ are the elemental mass matrix and constraint force vector respectively.

If all nodal Cartesian coordinates are collected in vector $\mathbf{q}_E \in \mathbb{R}^n$, all elemental contribution are assembled, and constraints $\boldsymbol{\Phi}_E$ are applied, the following general expression is obtained,

$$\delta\mathbf{q}_E^{\mathrm{T}} \cdot (\mathbf{M}_E \cdot \ddot{\mathbf{q}}_E - \mathbf{f}_{\Phi_E} - \mathbf{f}_{\mathrm{int}} - \mathbf{Q}_E) = 0 \qquad \forall \delta\mathbf{q}_E \in \mathcal{V}^n, \tag{7}$$

where $\mathbf{M}_E$ is the mass matrix, $\mathbf{f}_\Phi$ is the constraint force vector, and vector $\mathbf{Q}_E$ contains the contributions of the external forces.

Defining a global coordinate vector $\mathbf{q}^{\mathrm{T}} \overset{\mathrm{def}}{=} (\mathbf{q}_R^{\mathrm{T}} \,|\, \mathbf{q}_E^{\mathrm{T}})$, an ordinary differential equation system accounting for both rigid and deformable bodies can be written from Eqs. (3) and (7) as

$$\underbrace{\left(\begin{array}{c|c} \mathbf{M}_{\mathrm{R}} & \mathbf{0} \\ \hline \mathbf{0} & \mathbf{M}_{\mathrm{E}} \end{array}\right)}_{\mathbf{M}} \underbrace{\left(\begin{array}{c} \ddot{\mathbf{q}}_{\mathrm{R}} \\ \hline \ddot{\mathbf{q}}_{\mathrm{E}} \end{array}\right)}_{\ddot{\mathbf{q}}} = \underbrace{\left(\begin{array}{c} \mathbf{f}_{\Phi_{\mathrm{R}}} \\ \hline \mathbf{f}_{\Phi_{\mathrm{E}}} \end{array}\right) + \left(\begin{array}{c} \mathbf{f}_{\Phi_{\mathrm{RE1}}} \\ \hline \mathbf{f}_{\Phi_{\mathrm{RE2}}} \end{array}\right)}_{\mathbf{f}_\Phi} + \underbrace{\left(\begin{array}{c} \mathbf{0} \\ \hline \mathbf{f}_{\mathrm{int}} \end{array}\right) + \left(\begin{array}{c} \mathbf{Q}_{\mathrm{R}} \\ \hline \mathbf{Q}_E \end{array}\right)}_{\mathbf{Q}} \tag{8}$$

where $\mathbf{f}_{\Phi_{\mathrm{RE}i}}$ are forces associated to constraints acting simultaneously over rigid and deformable bodies.

4. Energy-momentum algorithm

The system of equations (8) is highly non-linear and stiff because the high-frequency components introduced by the large penalty parameters. This numerical ill-conditioning represents a serious drawback for most of the traditional time-stepping schemes (linear multi-step methods, trapezoidal rule, mid-point rule, etc). However, energy-momentum methods have remarkable robustness while conserving by design the total energy and momentum in conservative systems.

The appropriate context for the design of such methods is the study of discrete Hamiltonian systems with symmetry, where both the Hamiltonian function (physically, the total energy) and the momentum mapping associated with the symplectic action of the rotation group SO(3) (physically, the total momentum) are first integrals of the motion.

A discrete Hamiltonian system is introduced directly from the discrete derivative concept [4, 5]. This can be understood as an approximation of the continuous derivative at the mid-point, such that energy and momentum are exactly conserved. As a result, the discrete conservation is enforced by design in the method.

In practice, the general expression of the energy-momentum method is very similar to the mid-point rule. This last method can be written as

$$\begin{aligned} \mathbf{M}(\dot{\mathbf{q}}_{n+1} - \dot{\mathbf{q}}_n) &= \Delta t\, \mathbf{f}_{n+\frac{1}{2}}\,, \\ \frac{1}{2}(\dot{\mathbf{q}}_{n+1} + \dot{\mathbf{q}}_n) &= \frac{\mathbf{q}_{n+1} - \mathbf{q}_n}{h}\,, \end{aligned}$$

where $(\cdot)_{n+\frac{1}{2}}$ represents evaluation at the mid-point. The key idea is that the energy-momentum method substitutes $\mathbf{f}_{n+\frac{1}{2}}$ by force $\mathbf{f}^*$ such that energy and momentum are exactly conserved. The specific expression of $\mathbf{f}^*$ depends on the nature of the force: constraint ($\mathbf{f}_\Phi^*$), internal force ($\mathbf{f}_{\mathrm{int}}^*$) of a deformable body, external force ($\mathbf{f}_{\mathrm{ext}}^*$), contact force ($\mathbf{f}_c^*$), etc.

Expressions for the constraint force vectors $\mathbf{f}_\Phi^*$ and internal forces vectors $\mathbf{f}_{\mathrm{int}}^*$ are presented next. More details and expressions for external and contact forces can be found in [2, 3, 6].

Constraints

Consider first a general holonomic constraint Φ acting over several points with cartesian coordinate vectors $\mathbf{q}$. We call this type of constraint, where Φ depends on vector $\mathbf{q}$ in an arbitrary way, a *vector constraint*. It can be shown [3] that the constraint force $\mathbf{f}^*_\Phi$ in this case has the form

$$\mathbf{f}^*_\Phi = \alpha \overline{\Phi}_{n+\frac{1}{2}} (\mathrm{D}\Phi)_{n+\beta}\,.$$

In this expression, α is the penalty parameter, $\overline{\Phi}_{n+\frac{1}{2}}$ is the average of the constraint, such that

$$\overline{(\cdot)}_{n+\frac{1}{2}} \stackrel{\text{def}}{=} \frac{1}{2}\left[(\cdot)_n + (\cdot)_{n+1}\right],$$

and $(\mathrm{D}\Phi)_\beta$ is the gradient of the constraint evaluated at $\mathbf{q}_{n+\beta} \stackrel{\text{def}}{=} \mathbf{q}_n + \beta(\mathbf{q}_{n+1} - \mathbf{q}_n)$. The scalar β is calculated using the following iterative scheme,

$$\begin{aligned} \beta_{k+1} &= \beta_k - \frac{1}{\mathrm{D}\Psi(\beta_k)}\,\Psi(\beta_k), \\ \Psi(\beta) &\stackrel{\text{def}}{=} (\mathrm{D}\Phi)^{\mathrm{T}}_{n+\beta} \cdot (\mathbf{q}_{n+1} - \mathbf{q}_n) - \Phi_{n+1} + \Phi_n\,. \end{aligned} \tag{9}$$

If constraint Φ is at most quadratic, it can be shown that $\beta = \frac{1}{2}$, and the iterative scheme given by (9) is no longer necessary.

There are yet other types of constraints, the *scalar constraints*. These constraints act at most over two points $(\boldsymbol{x}_1\,,\,\boldsymbol{x}_2)$, and depend only on the modulus of their relative distance $r = ||\boldsymbol{x}_2 - \boldsymbol{x}_1|| = ||\boldsymbol{r}||$. It can be shown that in this case the constraint force is given by the closed expression

$$\mathbf{f}^*_\Phi = \alpha\,\frac{\Phi^2_{n+1} - \Phi^2_n}{r^2_{n+1} - r^2_n} \begin{Bmatrix} \boldsymbol{r}_{n+\frac{1}{2}} \\ -\boldsymbol{r}_{n+\frac{1}{2}} \end{Bmatrix}; \qquad \boldsymbol{r}_{n+\frac{1}{2}} = \frac{1}{2}(\boldsymbol{r}_{n+1} + \boldsymbol{r}_n).$$

Scalar constraints are extensively used for rigid body definition: each body is represented by four points and six constant-distance constraints that fall in this category.

Internal forces of elastic bodies

We study the case of deformable bodies with hyperelastic behaviour, such that there exists an energy density function (W) that verifies the following condition,

$$\boldsymbol{S} = 2\,\frac{\partial W(\boldsymbol{C}, \boldsymbol{X})}{\partial \boldsymbol{C}}\,,$$

where $\boldsymbol{S}$ is the second Piola–Kirchhoff stress tensor, $\boldsymbol{C}$ is the right Cauchy–Green strain tensor and $\boldsymbol{X}$ are the material coordinates of the point where the stress and strain fields are calculated.

In order to accomplish exact energy and momentum conservation, the contribution of an element Ω^e to the total internal force vector, should be [5]

$$(\mathbf{f}^e_{\mathrm{int}})^* = \int_{\Omega^e_0} \overline{\mathbf{B}}_{n+\frac{1}{2}} (\boldsymbol{S}^e)^*\,\mathrm{d}V_0$$

where:

$$\overline{\mathbf{B}}_{n+\frac{1}{2}} \stackrel{\text{def}}{=} \frac{\mathbf{B}_n + \mathbf{B}_{n+1}}{2}$$

$$(\boldsymbol{S}^e)^* \stackrel{\text{def}}{=} 2\left[(DW)_{n+\frac{1}{2}} + \frac{\Delta W - (\mathrm{D})_{n+\frac{1}{2}} : \Delta \boldsymbol{C}}{\Delta \boldsymbol{C} : \Delta \boldsymbol{C}} \Delta \boldsymbol{C}\right].$$

For a Saint Venant–Kirchhoff material, the second Piola–Kirchhoff stress tensor $\boldsymbol{S}$ and the Green–Lagrange strain tensor $\boldsymbol{E}$ are related through a constant fourth-order constitutive tensor $\mathbb{C}$, such that $\boldsymbol{S} = \mathbb{C} : \boldsymbol{E}$. In this specific case, the approximation of the middle-point stress $\boldsymbol{S}^*$ is particularly simple [7],

$$\boldsymbol{S}^* = \overline{\boldsymbol{S}}_{n+\frac{1}{2}} \stackrel{\text{def}}{=} \frac{1}{2}(\boldsymbol{S}_n + \boldsymbol{S}_{n+1}).$$

5. Representative numerical applications

Compound spherical pendulum

This application shows the performance of the method applied to a system of discrete particles under scalar and vector constraints.

The system is composed by two masses $m_A = m_B = 1$ kg constrained to move at constant distance and aligned with a fixed point O (Fig. 1). The system is parametrised by a vector $\mathbf{q}$ that contains the six Cartesian coordinates of the masses. Four independent constraints are defined. Two of them scalar (constant distance constraints) and the other two are vectorial (alignment of the masses with the origin).

Figure 2 shows the maximum time-step achieved by different methods for various penalty factors, for a total integration time of $T = 60$ s. The energy-momentum method presents the most robust

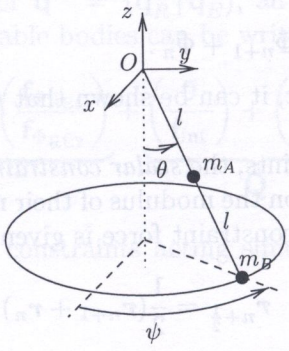

Fig. 1. Compound spherical pendulum

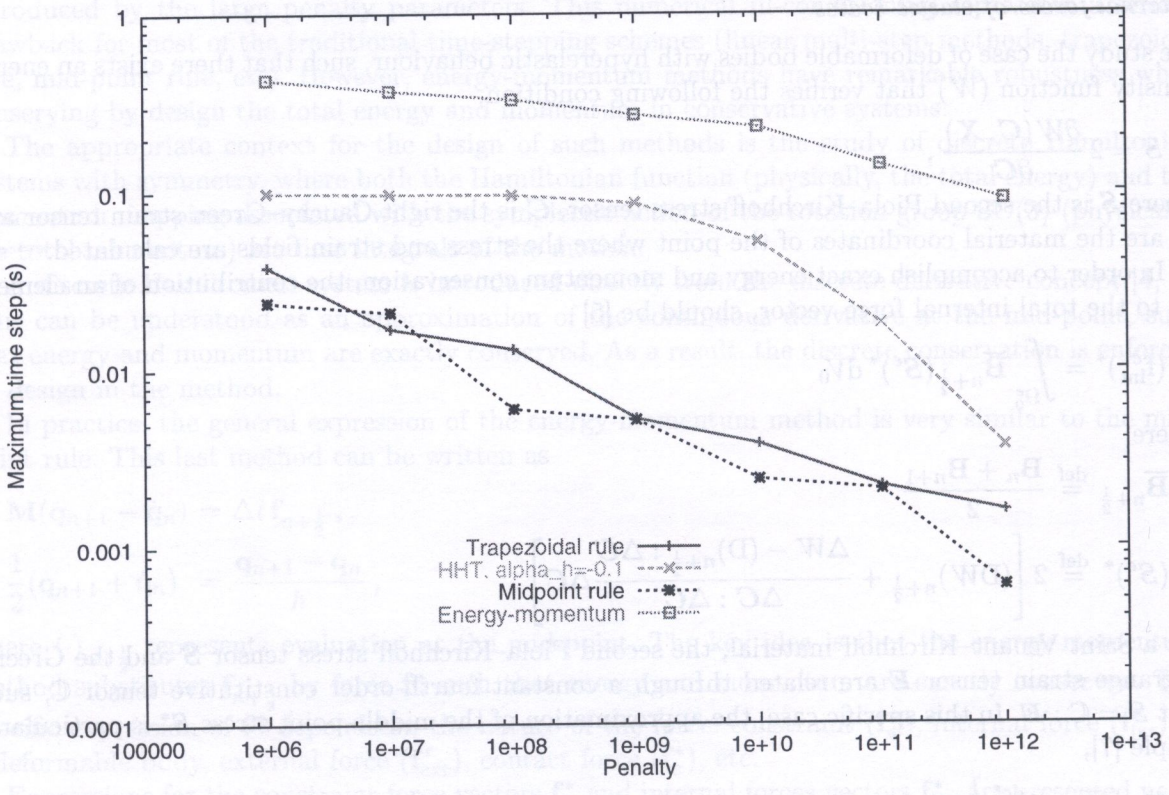

Fig. 2. Compound pendulum. Maximum time step vs. penalty factor

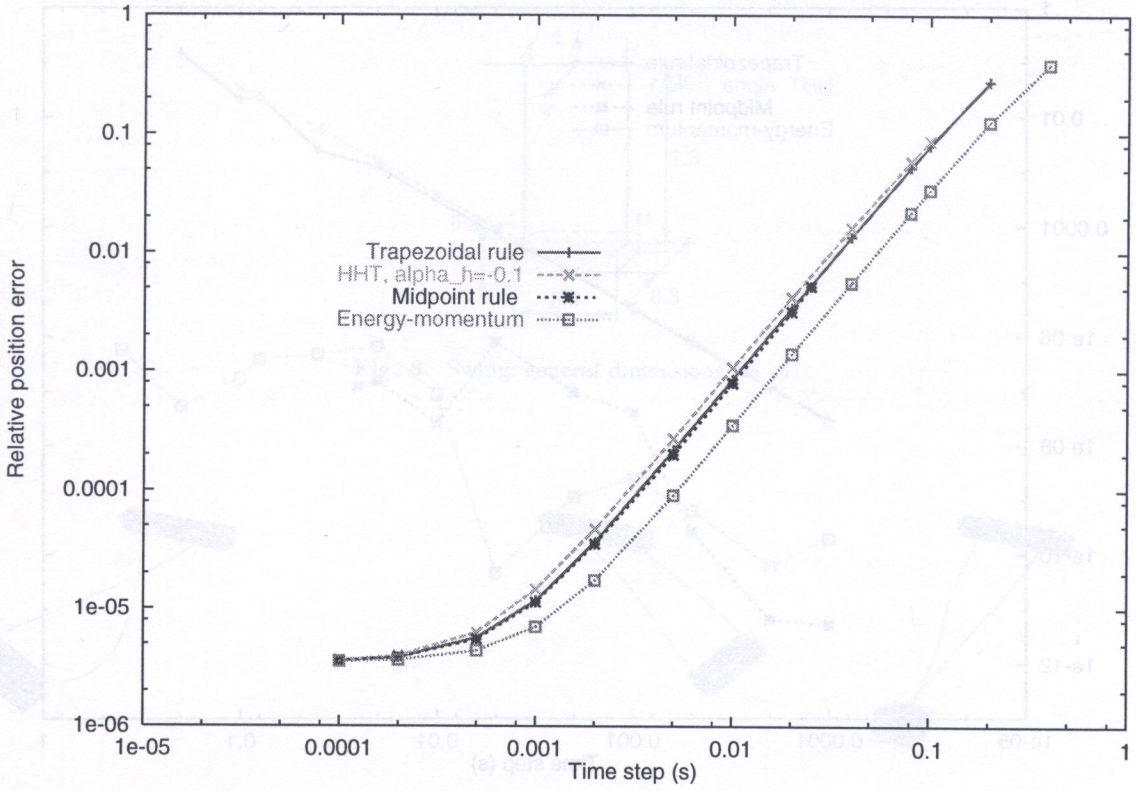

Fig. 3. Compound pendulum. Position relative error (ϵ_p) at $T = 2$ s, penalty factor $\alpha = 10^7$

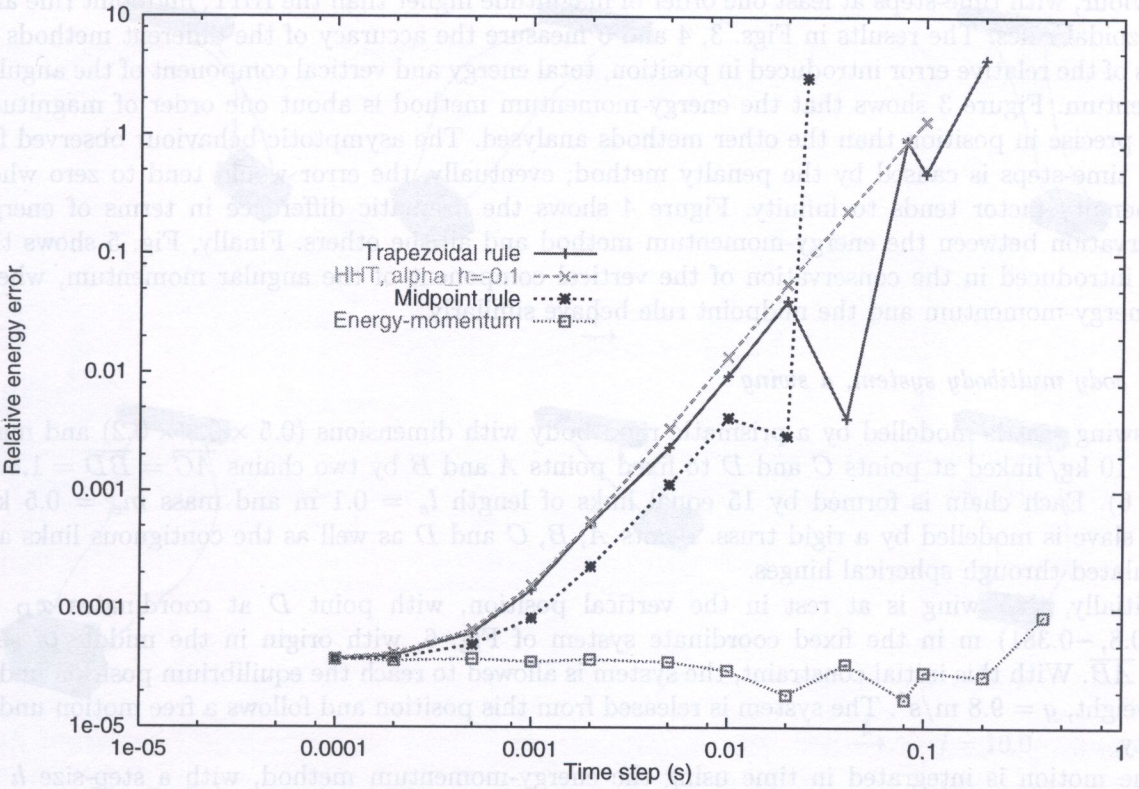

Fig. 4. Compound pendulum. Energy relative error (ϵ_p) at $T = 2$ s, penalty factor $\alpha = 10^7$

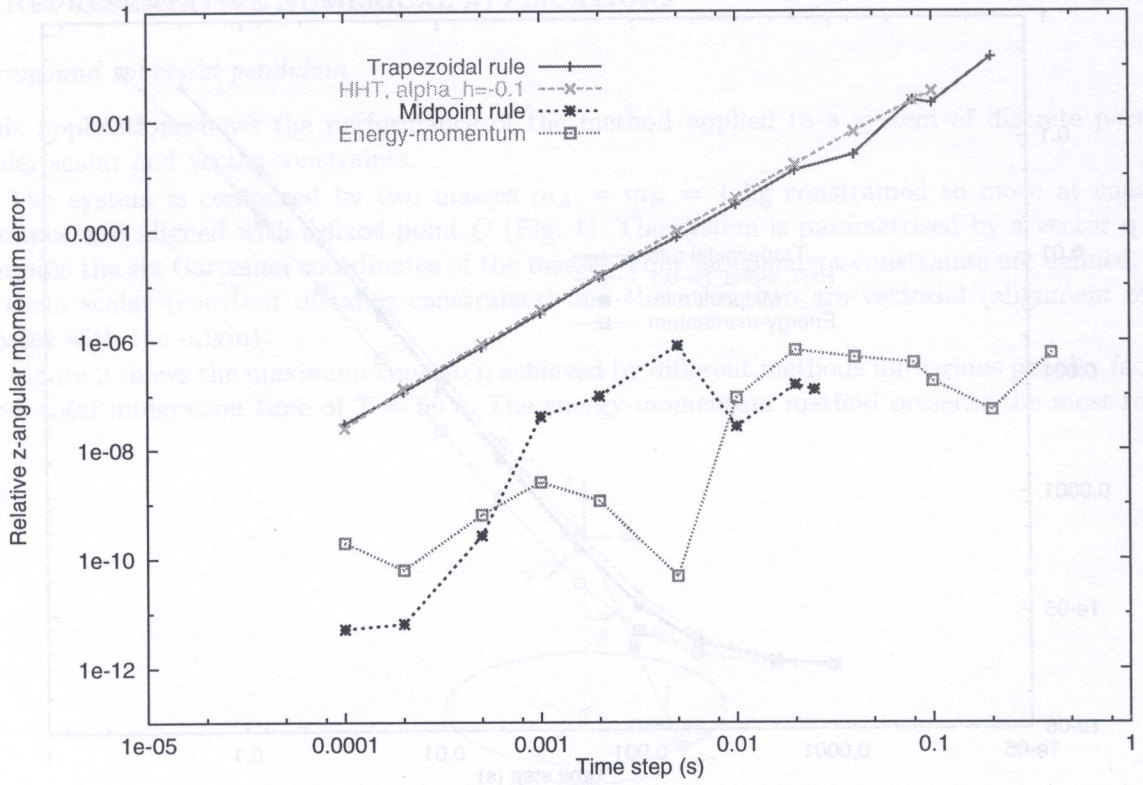

Fig. 5. Compound pendulum. Vertical angular momentum relative error (ϵ_p) at $T = 2$ s, penalty factor $\alpha = 10^7$

behaviour, with time-steps at least one order of magnitude higher than the HHT, midpoint rule and trapezoidal rules. The results in Figs. 3, 4 and 5 measure the accuracy of the different methods in terms of the relative error introduced in position, total energy and vertical component of the angular momentum. Figure 3 shows that the energy-momentum method is about one order of magnitude more precise in position than the other methods analysed. The asymptotic behaviour observed for small time-steps is caused by the penalty method; eventually, the error would tend to zero when the penalty factor tends to infinity. Figure 4 shows the dramatic difference in terms of energy conservation between the energy-momentum method and all the others. Finally, Fig. 5 shows the error introduced in the conservation of the vertical component of the angular momentum, where the energy-momentum and the midpoint rule behave similarly.

Rigid body multibody system, a swing

The swing seat is modelled by a prismatic rigid body with dimensions $(0.5 \times 0.3 \times 0.2)$ and mass $m_b = 10$ kg, linked at points C and D to fixed points A and B by two chains $\overline{AC} = \overline{BD} = 1.5$ m (Fig. 6). Each chain is formed by 15 equal links of length $l_e = 0.1$ m and mass $m_e = 0.5$ kg. Each slave is modelled by a rigid truss. Points A, B, C and D as well as the contiguous links are articulated through spherical hinges.

Initially, the swing is at rest in the vertical position, with point D at coordinates $\boldsymbol{x}_D = (1, -0.8, -0.381)$ m in the fixed coordinate system of Fig. 6, with origin in the middle of segment $\overline{AB}$. With this initial constraint, the system is allowed to reach the equilibrium position under self-weight, $g = 9.8$ m/s^2. The system is released from this position and follows a free motion under gravity.

The motion is integrated in time using the energy-momentum method, with a step-size $h = 0.002$ s over 10 s. The penalty parameter is set to $\alpha = 10^{10}$. The trapezoidal and midpoint rules and the Hilber, Hughes and Taylor (HHT) method have been tested also. Apart from the energy-

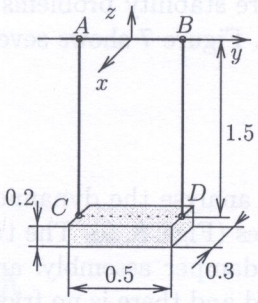

Fig. 6. Swing: general dimensions (in m)

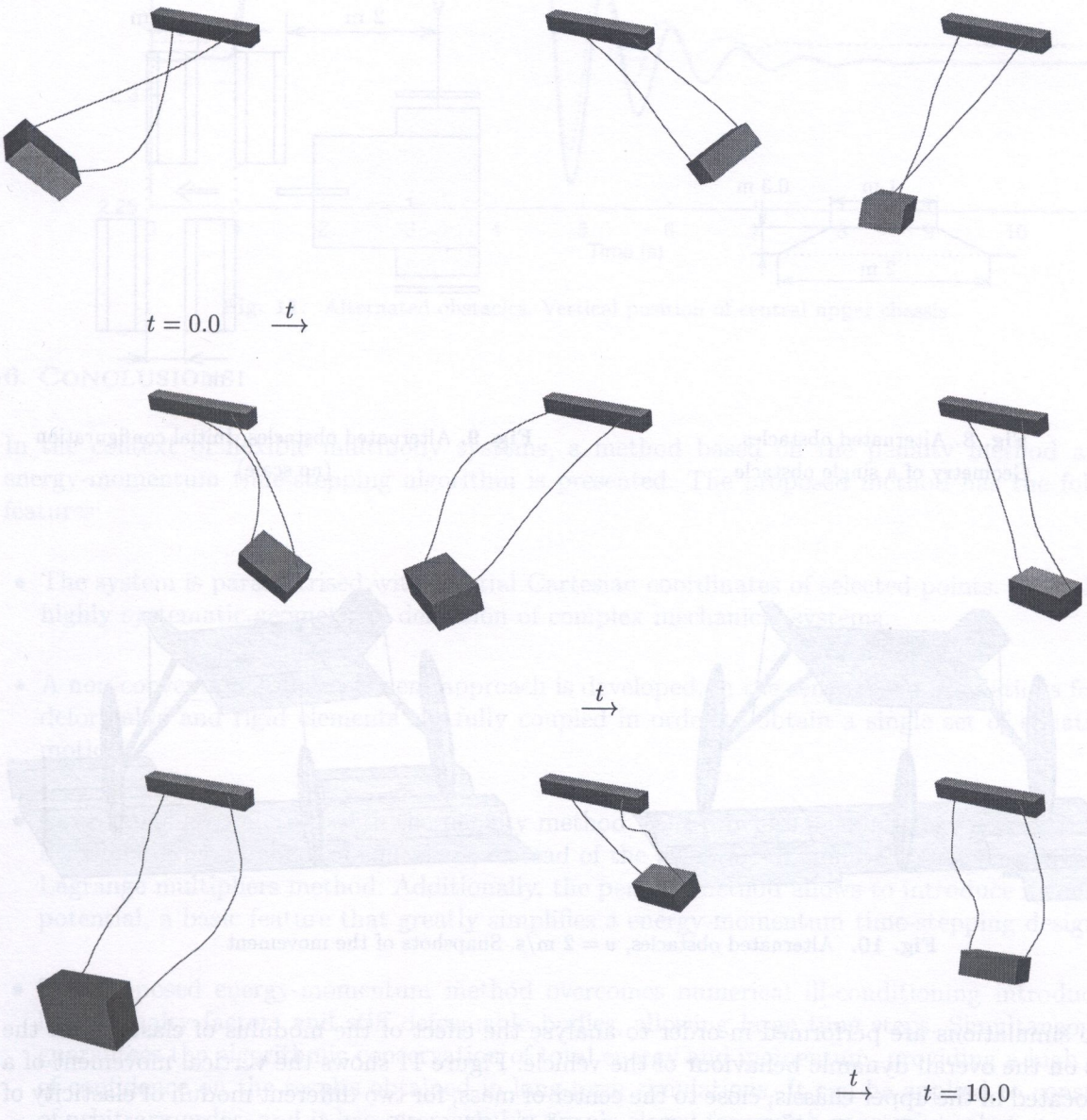

Fig. 7. Swing: snapshots of the movement (time flows from left to right and downwards)

momentum method, only the HHT with a damping parameter $\alpha_h = -0.2$, did successfully complete the integration up to 10 s without severe stability problems. However, HHT stability is associated with a substantial dissipation of energy. Figure 7 shows several snapshots of the movement.

Three-wheel vehicle

The main goal of this application is to analyse the dynamic behaviour of a simplified three-wheel vehicle over an alternated set of obstacles (Figs. 8, 9). The two rear wheels are linked to the chassis with McPherson struts, with a spring-damper assembly. and the flexible chassis is discretised in 20 elements. The wheels are not powered and there is no friction in any moving part. Details on the dimensions, mass distribution and mechanical properties of the materials can be found in [3]. The vehicle is launched against a double row of prismatic obstacles with a velocity of $v = 2$ m/s. Two snapshots of the movement are shown in Fig. 10.

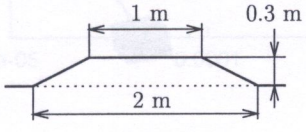

Fig. 8. Alternated obstacles. Geometry of a single obstacle

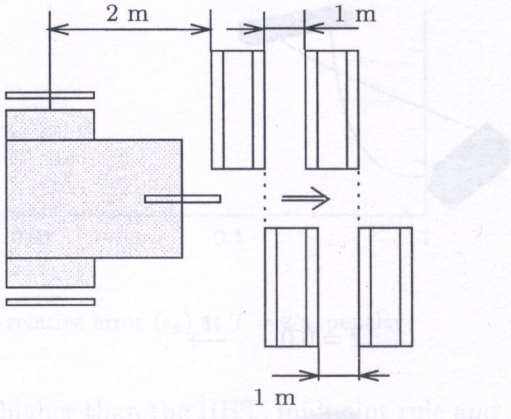

Fig. 9. Alternated obstacles. Initial configuration (no scale)

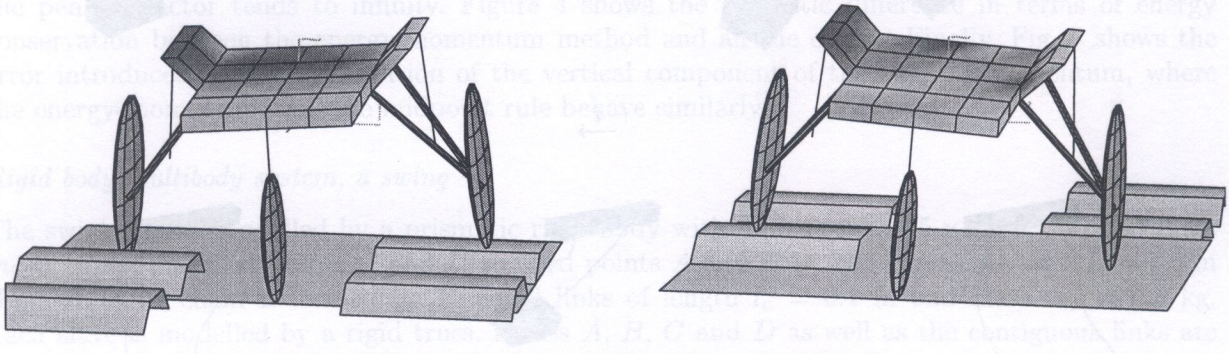

Fig. 10. Alternated obstacles, $v = 2$ m/s. Snapshots of the movement

Two simulations are performed in order to analyse the effect of the modulus of elasticity of the chassis on the overall dynamic behaviour of the vehicle. Figure 11 shows the vertical movement of a point located in the upper chassis, close to the center of mass, for two different moduli of elasticity of the chassis material, $E_1 = 2 \cdot 10^7$ Pa and $E_2 = 2 \cdot 10^8$ Pa. The stiffer chassis reaches the equilibrium position in a shorter period of time, as the velocity of the stress waves is higher in this case and the dissipation of energy through the dampers is faster.

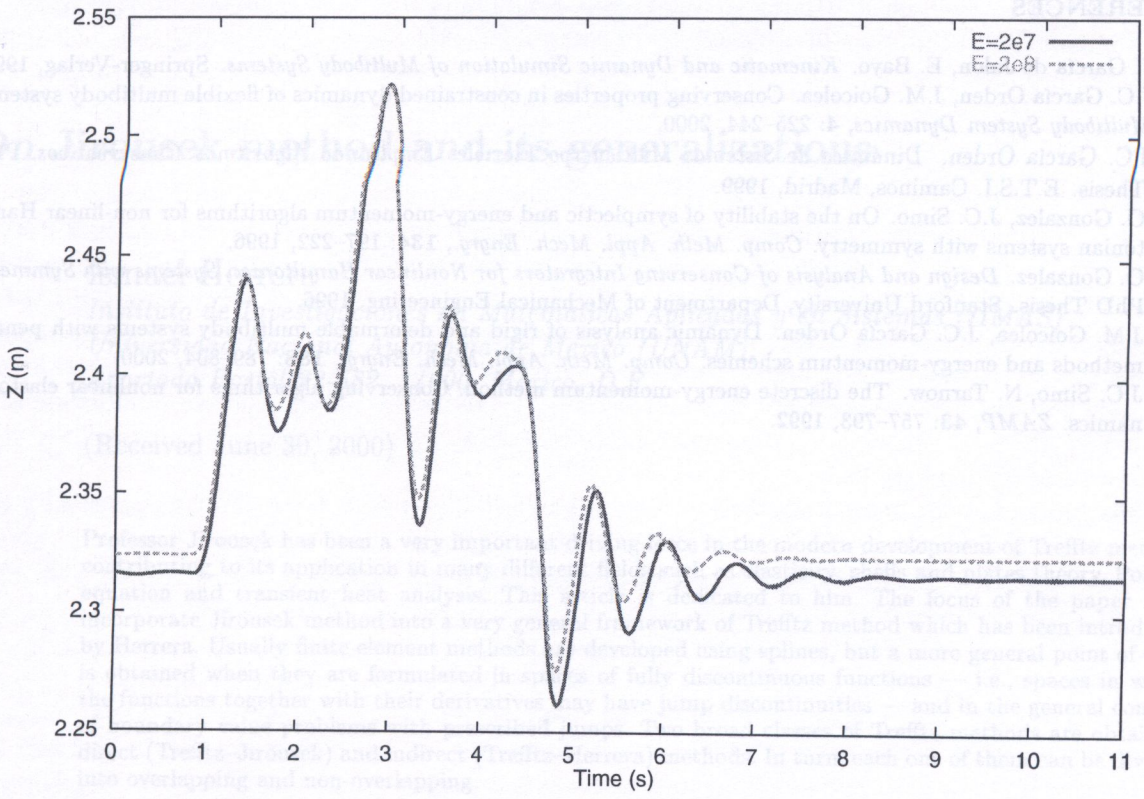

Fig. 11. Alternated obstacles. Vertical position of central upper chassis

6. Conclusions

In the context of flexible multibody systems, a method based on the penalty method and the energy-momentum time-stepping algorithm is presented. The proposed method has the following features:

- The system is parametrised with inertial Cartesian coordinates of selected points. This allows a highly systematic geometrical definition of complex mechanical systems.
- A non-conventional finite element approach is developed, in the sense that formulations for both deformable and rigid elements are fully coupled in order to obtain a single set of equations of motion.
- Constraints are enforced with the penalty method, that provides a simple formulation based on a strictly differential set of equations, instead of the algebraic-differential type generated by the Lagrange multipliers method. Additionally, the penalty method allows to introduce a constraint potential, a basic feature that greatly simplifies a energy-momentum time-stepping design.
- The proposed energy-momentum method overcomes numerical ill-conditioning introduced by large penalty factors and stiff deformable bodies, allowing large time steps. Simultaneously, it guarantees the algorithmic conservation of total energy and momentum, providing a high degree of confidence on the results obtained in long-term simulations. It can be applied to constraints of arbitrary order, and it has a remarkable simple closed form with constraints that are at most quadratic or depend on the modulus of the relative distance between two points.

REFERENCES

[1] J. García de Jalon, E. Bayo. *Kinematic and Dynamic Simulation of Multibody Systems.* Springer-Verlag, 1994.

[2] J.C. García Orden, J.M. Goicolea. Conserving properties in constrained dynamics of flexible multibody systems. *Multibody System Dynamics*, **4**: 225–244, 2000.

[3] J.C. García Orden, *Dinámica de Sistemas Multicuerpo Flexibles Empleando Algoritmos Conservativos.* PhD Thesis. E.T.S.I. Caminos, Madrid, 1999.

[4] O. Gonzalez, J.C. Simo. On the stability of symplectic and energy-momentum algorithms for non-linear Hamiltonian systems with symmetry. *Comp. Meth. Appl. Mech. Engrg.*, **134**: 197–222, 1996.

[5] O. Gonzalez. *Design and Analysis of Conserving Integrators for Nonlinear Hamiltonian Systems with Symmetry.* PhD Thesis. Stanford University, Department of Mechanical Engineering, 1996.

[6] J.M. Goicolea, J.C. García Orden. Dynamic analysis of rigid and deformable multibody systems with penalty methods and energy-momentum schemes. *Comp. Meth. Appl. Mech. Engrg.*, **188**: 789–804, 2000.

[7] J.C. Simo, N. Tarnow. The discrete energy-momentum method. Conserving algorithms for nonlinear elastodynamics. *ZAMP*, **43**: 757–793, 1992.